Supplementary Information File for:

Formation of amorphous molybdenum sulfide in abiotic and biotic sulfidic conditions: A comparative study on molybdenum sequestration mechanisms

Rachel F. Phillips[1,2,*], Weinan Leng[3], Sheryl A. Singerling[3,4], Morgane Desmau[5], and Jie Xu[1,*]

[1]School of Molecular Sciences, Arizona State University, Tempe, AZ, USA.

[2]School of Earth, Ocean and Environment, University of South Carolina, Columbia, SC, USA.

[3]The National Center for Earth and Environmental Nanotechnology Infrastructure, Virginia Tech, Blacksburg, VA, USA.

[4]Schwiete Cosmochemistry Laboratory, Goethe University, Frankfurt, Germany.

[5]Canadian Light Source, University of Saskatchewan, Saskatoon SK, Canada.

*Correspondence should be sent to rp66@mailbox.sc.edu or jiexu10@asu.edu

Table S1. SRB culture media recipes. All reagents used were ACS grade or higher. Initially, healthy cultures of *D. vulgaris* and *D. balticum* were grown in Postgate-63 and 1250 media, respectively. Once the exponential growth phase was reach in these cultures, 1 ml (1 %) of each was inoculated into their respective MTM media for growth and subsequent experimental addition of Mo as either MoO_4^{2-} or MoS_4^{2-} (and in some cases, Fe^{2+}).

***D vulgaris* media**	Media name: **Postgate-63**		**Dv-MTM**	
	g/L	**mM**	**g/L**	**mM**
NH_4Cl	1.0	18.69	1.0	18.69
NaCl	-	-	-	-
$MgSO_4 \cdot 7H_2O$	2.0	7.56	1.0	3.78
Na_2SO_4	1.0	7.04	2.3	16.20
KH_2PO_4	0.5	2.87	-	
$CaCl_2 \cdot 2H_2O$	0.1	0.68	0.06	0.41
HEPES	-	-	2.83	11.89
80% lactic acid	1.67	14.84	3.8	33.78
Yeast extract	1.0	-	0.05	-
$FeSO_4.7H_2O$	0.5	1.80	-	-
Na-thioglycolate	0.1	0.88	-	-
Ascorbic acid	0.1	0.57	-	-
Ionic strength =	0.09		0.13	
***D.balticum* media**	Media name: **1250**		**Db-MTM**	
	g/L	**mM**	**g/L**	**mM**
NH_4Cl	1.0	18.69	1.0	18.69
NaCl	24.3	416.40	24.3	416.10
Sodium citrate	5.0	19.38	-	-
$MgSO_4 \cdot 7H_2O$	4.4	16.61	4.4	16.64
Na_2SO_4	0.8	5.81	1.5	10.56
KH_2PO_4	0.5	2.87	-	-
$CaCl_2 \cdot 2H_2O$	0.9	6.12	0.9	6.12
HEPES	-	-	2.83	11.89
80% lactic acid	3.5	31.25	3.8	33.78
Yeast extract	1.0	-	0.05	-
Mohr's salt	1.0	2.55	-	-
Ionic strength =	0.59		0.75	

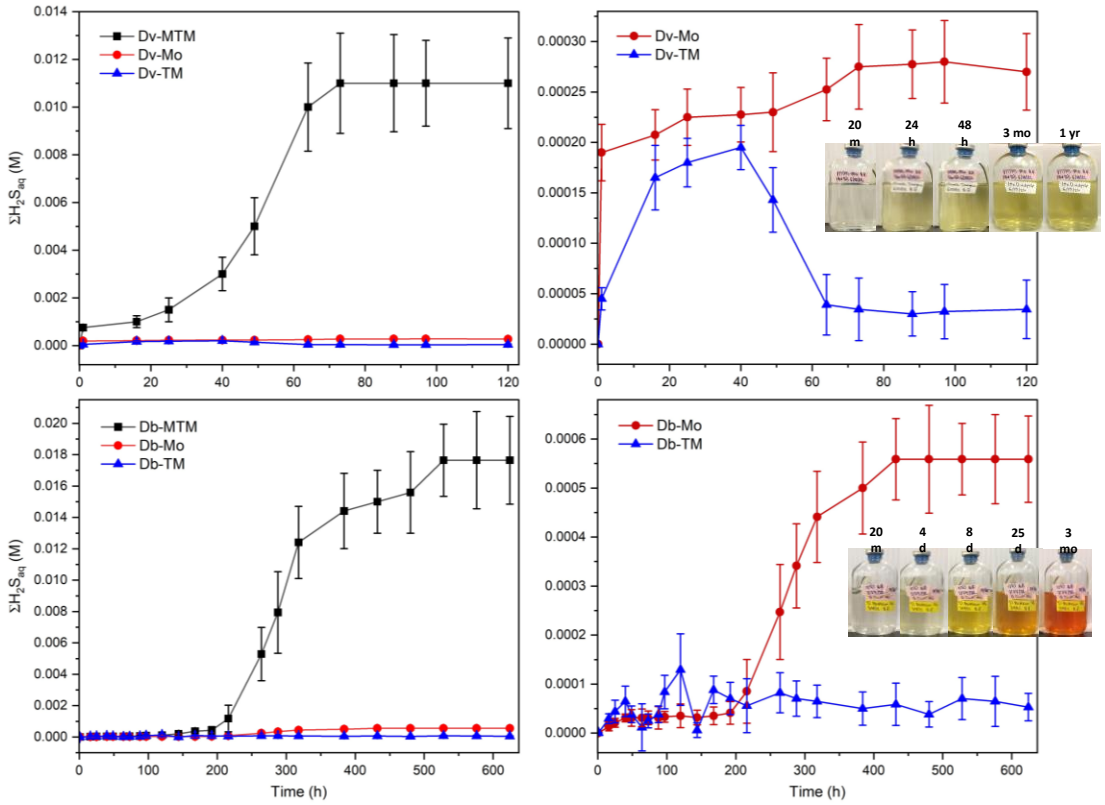

Figure S1. Sulfide production (growth) curves for D. vulgaris (Dv) and D balticum (Db) in the presence of MoO_4^{2-} (Mo) and MoS_4^{2-} (TM) compared to the absence of Mo (MTM).

Table S2. Thiolation and sequestration timing data (UV-vis).

Sample	Fe:Mo (initial)	Initial pH[a]	Ionic Strength (M)	Mo (mM)	Fe (mM)	Full thiolation (h)[b]	Full sequestration (h)[c]	Final pH[d]
Abiotic FeMoS experiments (from low to high pH)	1.00	7.57	0.01	0.5	0.5	72	700	7.73
	-	7.57	0.01	0.5	0.0	500	*No precipitates*	7.70
	1.00	4.34	0.01	0.5	0.5	0.5	96	4.33
	1.00	10.97	0.01	0.5	0.0	*Did not reach*	*Did not reach*	10.96
[Fe] Series: Live *D. vulagris* cultures	~0.03[e]	6.81	0.1	0.5	0.0	120	*Did not reach*	7.12
	0.50	6.88	0.1	0.5	0.5	5	600	7.36
	1.00	6.91	0.1	0.5	0.5	1.5	72	7.32
	2.00	6.82	0.1	0.5	0.5	0.5	30	7.29
[Fe] Series: Uninoculated *D. vulgaris* media	-	7.21	0.1	0.5	0.0	1000	*No precipitates*	7.53
	0.02	7.20	0.1	0.5	0.01	350	*Did not reach*	7.29
	0.10	7.31	0.1	0.5	0.05	*not measured*	*Did not reach*	7.40
	0.50	7.17	0.1	0.5	0.5	24	~4500	7.23
	1.00	7.19	0.1	0.5	0.5	10	850	7.56
	2.00	7.12	0.1	0.5	0.5	12	120	7.14
[Fe] Series: Live *D. balticum* cultures	~0.03[e]	7.75	0.7	0.5	0.0	~6000	*Did not reach*	8.31
	0.50	7.57	0.7	0.5	0.5	250	*Did not reach*	7.76
	1.00	7.55	0.7	0.5	0.5	150	~3000	7.69
	2.00	7.56	0.7	0.5	0.5	72	300	7.79
[Fe] Series: Uninoculated *D. balticum* media	-	7.95	0.7	0.5	0.0	~6000	*No precipitates*	8.18
	0.50	7.89	0.7	0.5	0.5	900	*Did not reach*	7.92
	1.00	7.92	0.7	0.5	0.5	250	~3500	7.99
	2.00	7.88	0.7	0.5	0.5	72	300	7.97

[a]Initial pH was taken after autoclaving and 5mM sulfide addition/production.
[b]Full thiolation refers to the time required for the initial MoO_4^{2-} to be completely converted to MoS_4^{2-} as indicated by the presence of MoS_4^{2-} peaks and absence of thiomolybdate intermediate peaks in UV-vis spectra.
[c]Full sequestration refers to the time required for the $MoO_xS_{4-x}^{2-}$ to be fully reduced and precipitated as indicated by the absence of $MoO_xS_{4-x}^{2-}$ peaks in UV-vis spectra.
[d]Final pH was taken from supernatant after aging (i.e., experimental duration).
[e]These experiments were initial meant to contain no Fe, but a small amount of Fe was transferred during inoculation of the media (see section 4.2 of main text).

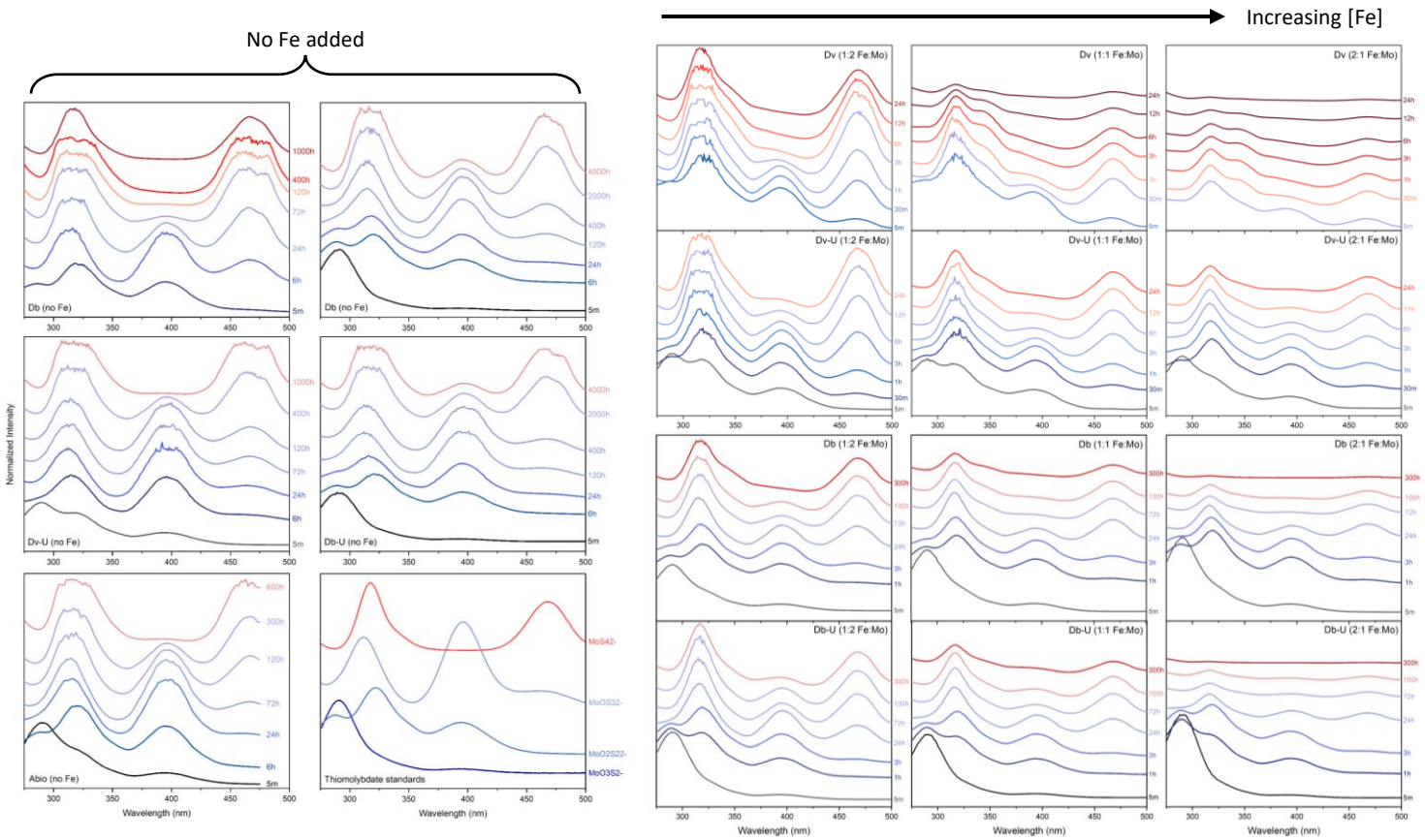

Figure S2. UV-vis spectra showing stepwise Mo thiolation in Fe-Mo-S solutions over the course of aging (up to ~4000 h or about 6 months, depending on the sample and its associated rate of Mo thiolation and sequestration). The left portion of this figure shows Mo thiolation in systems with no Fe added (at least not intentionally; see text for details), and the right side shows Mo thiolation in Fe-containing solutions. Dv = *D. vulgaris* cultures; Db = *D. balticum* cultures, Dv/Db-U = uninoculated *D. vulgaris/D. balticum* media.

Table S3. Final aqueous and precipitate Fe, Mo, S concentrations from ICP-OES and XPS analyses, respectively.

Sample	Experiment Duration[a]	Initial Fe:Mo_{aq}[b]	Initial pH[c]	Ionic Strength (M)	Final pH[d]	Final $[Mo]_{aq}$ (mM)[f]	Final $[Fe]_{aq}$ (mM)[f]	Final $[Mo]_s$ (%)	Final $[Fe]_s$ (%)	Final $[S]_s$ (%)	Final Fe:Mo_s[g]
Abiotic FeMoS experiments (from low to high pH)	40+ d	1.00	4.34	0.01	4.33	0.0000	0.0047	1.00	1.70	8.40	1.70
	40+ d	1.00	7.57	0.01	7.73	0.0204	0.0082	3.00	1.20	25.40	0.40
	40+ d	1.00	10.97	0.01	10.96	1.0138	0.1069	0.60	9.00	11.90	15.0
Dv[e]-L (Fe+Mo added before inoc.)	~30 d	1.00	6.71[e]	0.1	6.88	-	-	0.50	0.80	2.70	1.60
Dv-L (Mo added before inoc.)	~30 d	1.00	6.67[e]	0.1	7.01	-	-	2.90	1.90	9.10	0.66
Dv-D (Fe+Mo added to dead cell culture)	~30 d	1.00	6.71[e]	0.1	6.89	-	-	2.60	3.20	11.60	1.23
Db-L (Fe+Mo added before inoc.)	~30 d	1.00	7.38[e]	0.7	7.45	-	-	9.30	5.50	22.10	0.59
Time Series: Live *D. vulgaris* cultures	5 min	1.00	6.85	0.1	7.01	0.4689	0.8213	0.20	0.60	2.90	3.00
	3 h	1.00	6.78	0.1	6.99	0.3568	1.4872	0.30	1.40	3.60	4.70
	24 h	1.00	6.89	0.1	7.00	0.2563	1.2175	3.10	3.10	10.50	1.00
	4 d	1.00	6.80	0.1	7.12	0.0070	0.0023	-	-	-	-
	8 d	1.00	6.82	0.1	7.19	0.0004	0.0023	3.50	2.10	11.00	0.60
	40+ d	1.00	6.91	0.1	7.32	0.0002	0.0048	1.00	0.90	6.00	0.90
Time Series: Uninoculated *D. vulgaris* media	5 min	1.00	7.16	0.1	7.19	-	-	0.40	5.00	9.30	7.14
	3 h	1.00	7.17	0.1	7.18	-	-	0.70	5.00	15.00	12.5
	24 h	1.00	7.16	0.1	7.22	-	-	4.00	4.20	15.40	1.05
	4 d	1.00	7.20	0.1	7.29	-	-	-	-	-	-
	8 d	1.00	7.18	0.1	7.42	-	-	4.60	4.90	17.40	1.07
	40+ d	1.00	7.19	0.1	7.56	0.0233	0.0363	7.30	5.20	22.80	0.71
[Fe] Series: Live *D. vulgaris* cultures	160+ d	~0.03[e]	6.81	0.1	7.12	0.2196	0.0175	0.70	<0.10	3.00	≤0.14
	40+ d	0.50	6.88	0.1	7.36	0.0003	0.0116	2.60	0.80	8.40	0.31
	40+ d	1.00	6.91	0.1	7.32	0.0002	0.0048	1.00	0.90	6.00	0.90
	40+ d	2.00	6.82	0.1	7.29	0.0001	0.0011	1.30	1.40	7.10	1.08
[Fe] Series: Uninoculated *D. vulgaris* media	80+d	0.02	7.20	0.1	7.29	0.5495	0.0868	1.10	<0.10	7.60	≤0.09
	80+d	0.10	7.31	0.1	7.40	0.5195	0.1235	1.60	<0.10	10.80	≤0.06
	40+ d	0.50	7.17	0.1	7.23	0.2033	0.0774	6.20	4.20	21.50	0.68
	40+ d	1.00	7.19	0.1	7.56	0.0233	0.0363	7.30	5.20	22.80	0.71
	40+ d	2.00	7.12	0.1	7.14	0.0002	0.0029	4.70	6.60	24.10	1.40
[Fe] Series: Live *D. balticum* cultures	160+ d	~0.03[e]	7.75	0.7	8.31	-	-	-	-	-	-
	80+ d	0.50	7.57	0.7	7.76	0.1756	0.0548	2.00	1.30	9.10	0.65
	80+ d	1.00	7.55	0.7	7.69	0.0112	0.0106	3.10	2.10	11.50	0.68
	80+ d	2.00	7.56	0.7	7.79	0.0001	0.0014	1.90	2.70	10.00	1.42
[Fe] Series: Uninoculated *D. balticum* media	80+ d	0.50	7.89	0.7	7.92	0.1003	0.4312	6.40	4.80	23.60	0.75
	80+ d	1.00	7.92	0.7	7.99	0.0564	0.0152	7.00	5.00	23.00	0.71
	80+ d	2.00	7.88	0.7	7.97	0.0001	0.0025	4.40	4.60	19.40	1.05

[a]Experiments aged for 30+ days were stopped at what was interpreted as equilibrium based on 'full sequestration' (disappearance of thiomolybdate peaks in UV-vis spectra).
[b]All experiments were run with 0.5 mM initial $[Mo]_{aq}$ and 5 mM initial $[S]_{aq}$ (for inoculated cultures, initial S species was sulfate; for abiotic/uninoculated samples, initial S was sulfide). Initial $[Fe]_{aq}$ fluctuated between 0.015, 0.25, 0.5, and 1.0 mM to test different initial Fe:Mo ratios.
[c]Initial pH was taken after autoclaving and 5 mM sulfide addition/production.
[d]Final pH was taken from supernatant after aging (i.e., experimental duration).
[e]These experiments were initial meant to contain no Fe, but a small amount of Fe was transferred during inoculation of the media (see section 4.2 of main text).
[f]Note: Some final aqueous Mo and Fe concentrations are higher than the 0.5-1.0 mM starting concentrations due to a couple factors: (1) error associated w/ICP-OES measurements and (2) some evaporation likely occurred as samples were degassed in vent hood in preparation for ICP-OES, concentrating the Mo and Fe in solution.
[g]Note: The Fe:Mo_s ratios in the solid are mass ratios, whereas the initial aqueous Fe:Mo_{aq} ratios are based on molarity.

S1. Molybdenum XPS fitting parameters

High-resolution Mo3d XPS spectra were deconvoluted to determine the relative contribution of Mo(IV), Mo(V), and Mo(VI) in the FeMoS precipitates. Mo3d spectra were fit with one doublet at ~228.6 eV ($Mo3d_{5/2}$) and ~231.7 eV ($Mo3d_{3/2}$) corresponding to Mo(IV), another doublet at ~230.0 eV ($Mo3d_{5/2}$) and ~233.1 eV ($Mo3d_{3/2}$) corresponding to Mo(V), and a third doublet at ~232.3 eV ($Mo3d_{5/2}$) and ~235.4 eV ($Mo3d_{3/2}$) corresponding to Mo(VI) (Muijsers et al., 1995; Weber et al., 1996; Sanders et al., 1999; Herrera and Resasco, 2004; Qi et al., 2015; Weber et al., 2015 Seo et al., 2015; Seo et al., 2020; Miller et al., 2020; Phillips et al., 2023). The difference in binding energy between peaks in each doublet was set at 3.1 eV, the $Mo3d_{5/2}$ to $Mo3d_{3/2}$ peak area ratio was set to 1.5, and the full width half maximum (FWHM) was set at equal values for all peaks (Qi et al., 2015; Seo et al., 2015; Seo et al., 2020).

S2. Iron XPS fitting parameters

High resolution $Fe2p_{3/2}$ XPS spectra were fit with a single peak at ~707.5 eV corresponding to Fe(II)-S, a multiplet of four peaks at ~708.7, 709.7, 710.7, and 711.7 eV corresponding to Fe(III)-S, and, for some spectra, an additional peak at ~711.8 eV corresponding to Fe(III)-O (Herbert et al., 1998; Wan et al., 2014; Lan and Butler, 2016; Phillips et al., 2023). The FWHM was set at the same value for all peaks. The peak area ratios for the Fe(III)-S multiplet were set at 0.66, 0.35, and 0.11 relative to the largest peak at ~708.7 eV (Lan and Butler, 2016).

S3. Sulfur XPS fitting parameters

High resolution S2p XPS spectra were fit with a doublet at ~161.2 eV ($2p_{3/2}$) and ~162.4 eV ($2p_{1/2}$) representing monosulfide (S^{2-}), another doublet at ~161.9 eV ($2p_{3/2}$) and ~163.2 eV ($2p_{1/2}$) representing disulfide (S_2^{2-}), and a third doublet at ~163.0 eV ($2p_{3/2}$) and ~164.2 eV ($2p_{1/2}$) representing polysulfide (S_n^{2-}) (e.g., Karthe et al., 1993; Nesbitt and Muir; 1994; Nesbitt et al., 2000; Mullet et al., 2002; Poulton, 2003; Wan et al., 2014; Lan and Butler, 2016; Phillips et al., 2023). The $S2p_{1/2}$ to $S2p_{3/2}$ peak area ratios for each doublet were set to 1:2, and the FWHM was set at the same value for all peaks.

Table S4. Final precipitate Fe, Mo, S speciation results from high resolution XPS fitting.

Sample	Experiment Duration[a]	Initial Fe:Mo_{aq}[b]	Initial pH[c]	Ionic Strength (M)	Final pH[d]	% Mo(IV)	% Mo(V)	% Mo(VI)	% S^{2-}	% S_2^{2-}	% S_n^{2-}	% Fe(II)S	% Fe(III)S	% Fe(III)O
Abiotic FeMoS experiments (from low to high pH)	40+ d	1.00	7.57	0.01	7.73	90	10	0	45	55	0	-	-	-
	40+ d	1.00	4.34	0.01	4.33	81	19	0	64	9	27	54	46	0
	40+ d	1.00	10.97	0.01	10.96	-	-	-	68	10	22	42	52	6
Dv[e]-L (Fe+Mo added before inoc.)	~30 d	1.00	6.71[e]	0.1	6.88	78	22	0	35	41	24	47	47	7
Dv-L (Mo added before inoc.)	~30 d	1.00	6.67[e]	0.1	7.01	85	15	0	56	19	25	52	43	5
Dv-D (Fe+Mo added to dead cell culture)	~30 d	1.00	6.71[e]	0.1	6.89	80	20	0	52	18	30	56	40	4
Db-L (Fe+Mo added before inoc.)	~30 d	1.00	7.38[e]	0.7	7.45	83	17	0	69	13	18	56	40	4
Time Series: Live *D. vulgaris* cultures	5 min	1.00	6.85	0.1	7.01	50	19	31	52	34	14	19	66	15
	3 h	1.00	6.78	0.1	6.99	67	16	17	43	41	16	37	57	6
	24 h	1.00	6.89	0.1	7.00	84	16	0	71	14	15	60	38	2
	8 d	1.00	6.82	0.1	7.19	74	26	0	69	24	7	55	42	2
	40+ d	1.00	6.91	0.1	7.32	83	17	0	74	13	13	55	41	4
Time Series: Uninoculated *D. vulgaris* media	5 min	1.00	7.16	0.1	7.19	75	25	0	59	22	19	47	49	5
	3 h	1.00	7.17	0.1	7.18	88	12	0	53	31	16	54	43	3
	24 h	1.00	7.16	0.1	7.22	85	15	0	58	25	17	54	43	3
	8 d	1.00	7.18	0.1	7.42	82	18	0	63	27	10	57	42	1
	40+ d	1.00	7.19	0.1	7.56	82	18	0	66	18	16	59	39	2
[Fe] Series: Live *D. vulgaris* cultures	160+ d[g]	~0.03[f]	6.81	0.1	7.12	76	18	6	51	23	26	[h]	[h]	[h]
	40+ d	0.50	6.88	0.1	7.36	81	19	0	58	27	15	52	45	4
	40+ d	1.00	6.91	0.1	7.32	83	17	0	74	13	13	55	41	4
	40+ d	2.00	6.82	0.1	7.29	85	15	0	41	48	11	54	43	3
[**Fe] Series**: Uninoculated *D. vulgaris* media	80+d	0.02	7.20	0.1	7.29	56	17	27	50	38	12	[h]	[h]	[h]
	80+d	0.10	7.31	0.1	7.40	53	20	27	42	45	13	[h]	[h]	[h]
	40+ d[g]	0.50	7.17	0.1	7.23	87	13	0	55	16	30	46	48	7
	40+ d	1.00	7.19	0.1	7.56	82	18	0	66	18	16	59	39	2
	40+ d	2.00	7.12	0.1	7.14	75	25	0	67	1	32	49	47	4
[Fe] Series: Live *D. balticum* cultures	160+ d[g]	~0.03[f]	7.75	0.7	8.31	-	-	-	-	-	-	-	-	-
	80+ d[g]	0.50	7.57	0.7	7.76	72	14	14	51	22	27	46	46	8
	80+ d[g]	1.00	7.55	0.7	7.69	79	21	0	76	1	22	57	39	4
	80+ d	2.00	7.56	0.7	7.79	75	11	14	67	18	15	48	39	13
[Fe] Series: Uninoculated *D. balticum* media	80+ d	0.50	7.89	0.7	7.92	86	14	0	64	19	17	58	40	2
	80+ d	1.00	7.92	0.7	7.99	83	17	0	68	22	10	56	41	3
	80+ d	2.00	7.88	0.7	7.97	85	25	0	74	22	4	55	43	1

[a]All experiments run for 30 days or more were run to what was believed as equilibrium based on 'full sequestration' (i.e., disappearance of thiomolybdate peaks in UV-vis spectra).
[b]All experiments were run with 0.5 mM initial $[Mo]_{aq}$ and 5 mM initial $[S]_{aq}$ (for inoculated cultures, initial S species was sulfate; for abiotic/uninoculated samples, initial S was sulfide). Initial $[Fe]_{aq}$ fluctuated between 0.015, 0.25, 0.5, and 1.0 mM to test different initial Fe:Mo ratios.
[c]Initial pH was taken after autoclaving and 5 mM sulfide addition/production.
[d]Final pH was taken from supernatant after aging (i.e., experimental duration).
[e]Dv => D. vulgaris culture; Db => D. balticum culture.
[f]These experiments were initial meant to contain no Fe, but a small amount of Fe was transferred during inoculation of the media (see section 4.2 of main text).
*[g]Experiments that that may not have reached equilibrium**
[h]Not enough Fe in these precipitates to get high resolution data.

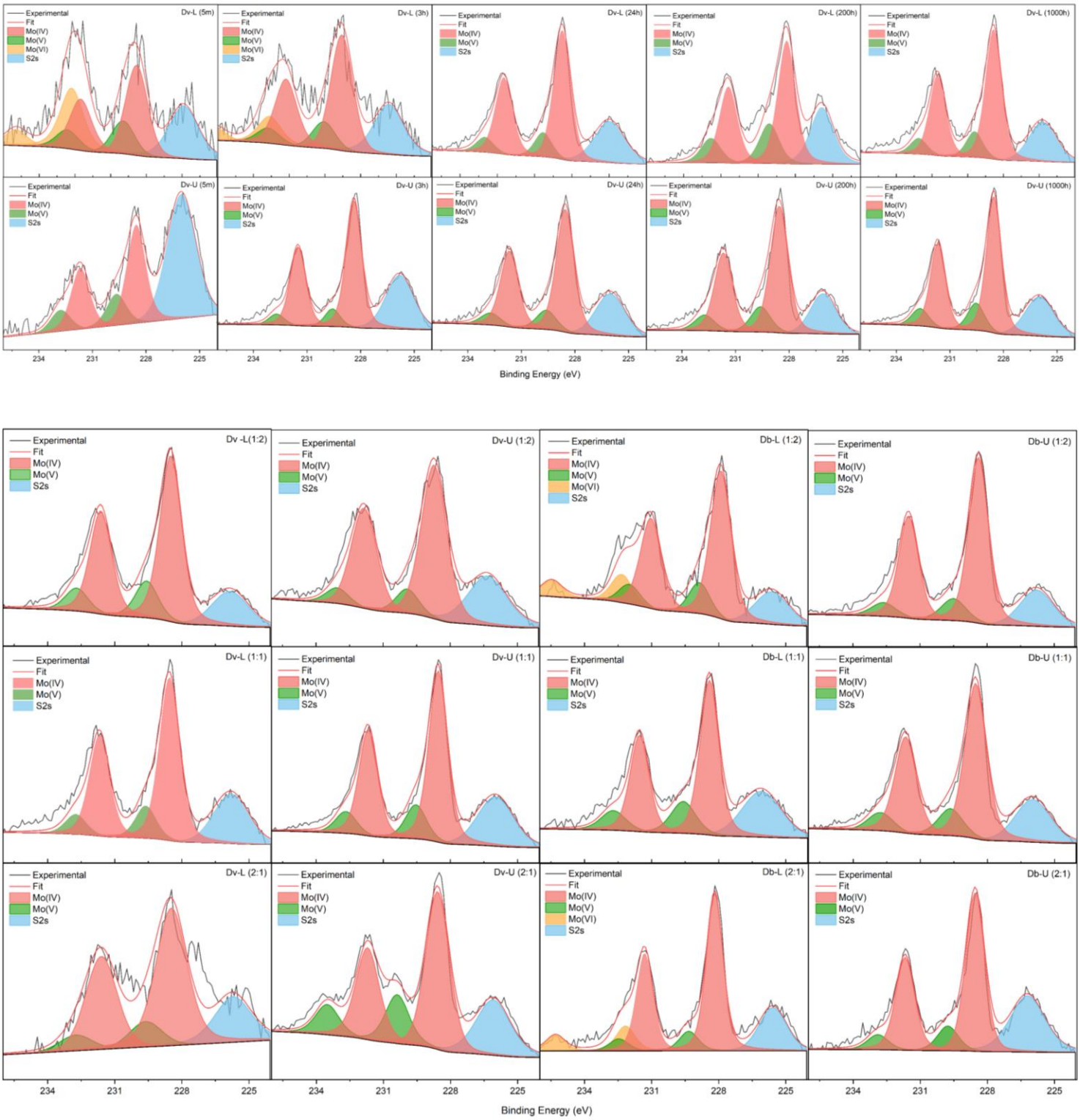

Figure S3. Best fits for high-resolution Mo3d XPS spectra for time series (top two rows) and [Fe] series (bottom 3 rows). Abbreviations: Dv-L => live *D. vulgaris* culture; Dv-U => uninoculated/abiotic *D. vulgaris* media; Db-L => live *D. balticum* culture; Db-U => uninoculated/abiotic *D. balticum* media. Fe to Mo ratios are 1:2, 1:1, or 2:1 as indicated for each sample in [Fe] series.

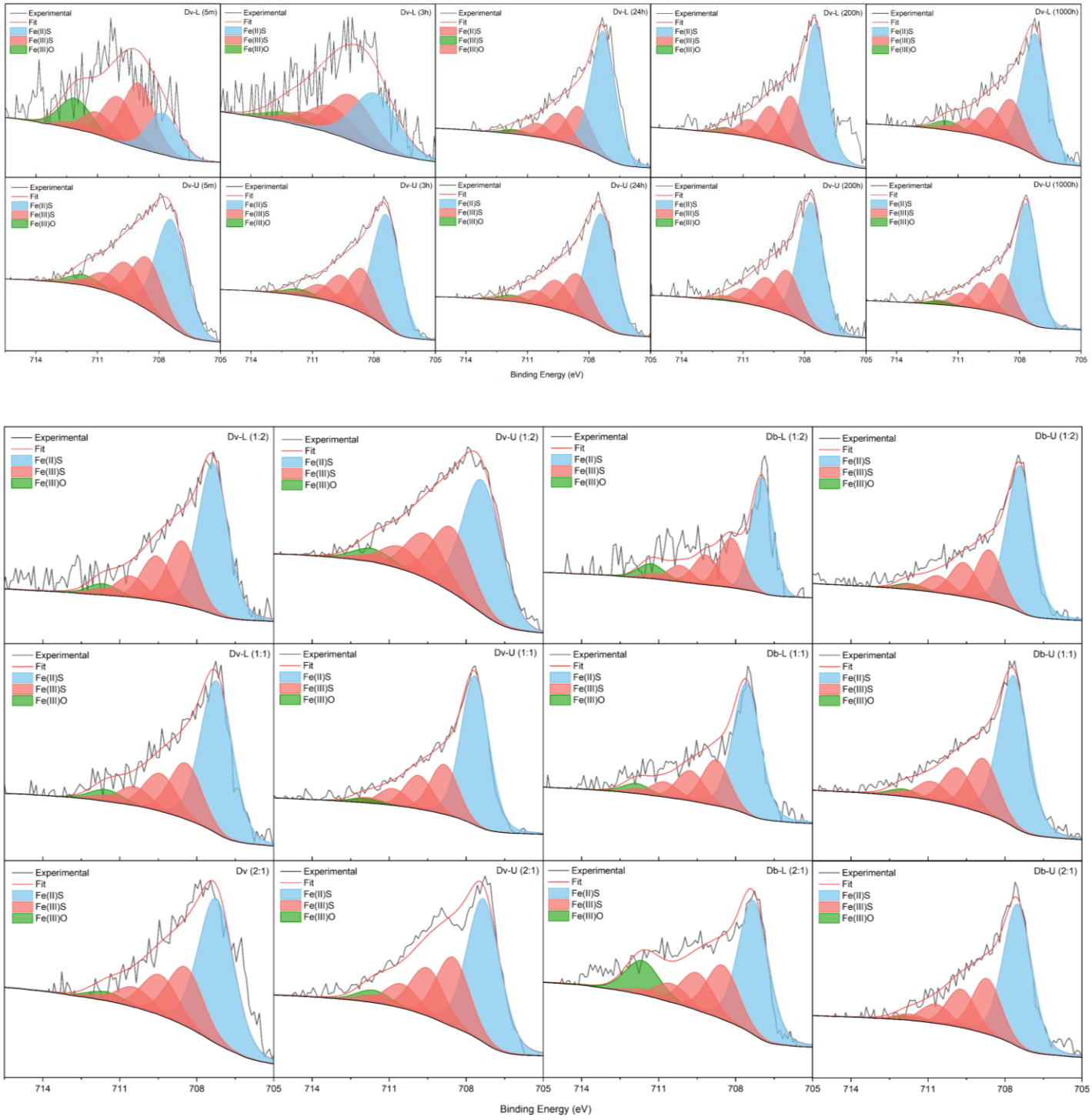

Figure S4. Best fits for high-resolution Fe2p XPS spectra for time series (top two rows) and [Fe] series (bottom 3 rows). Abbreviations: Dv-L => live *D. vulgaris* culture; Dv-U => uninoculated/abiotic *D. vulgaris* media; Db-L => live *D. balticum* culture; Db-U => uninoculated/abiotic *D. balticum* media. Fe to Mo ratios are 1:2, 1:1, or 2:1 as indicated for each sample in [Fe] series.

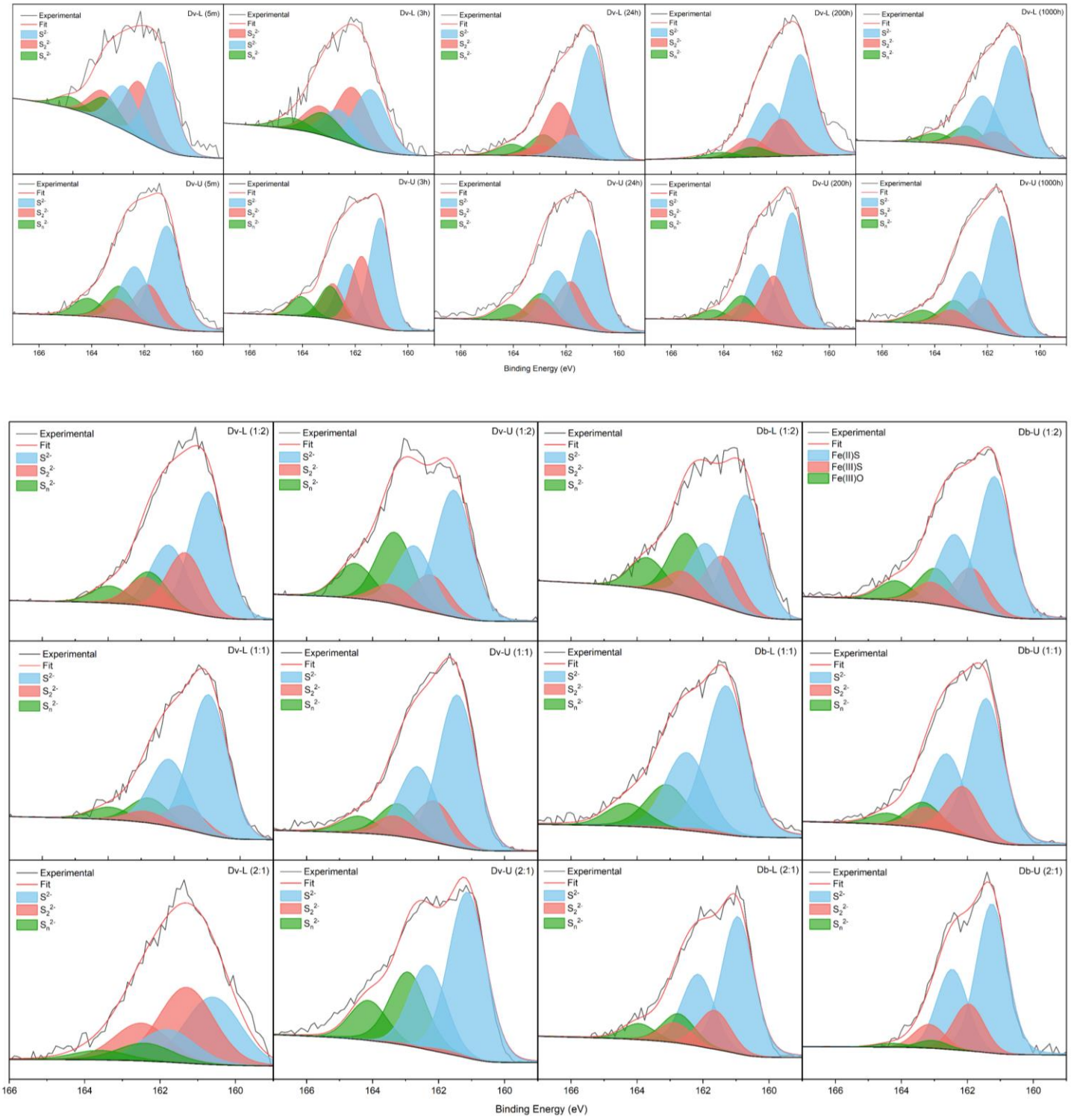

Figure S5. Best fits for high-resolution S2p XPS spectra for time series (top two rows) and [Fe] series (bottom 3 rows). Abbreviations: Dv-L => live *D. vulgaris* culture; Dv-U => uninoculated/abiotic *D. vulgaris* media; Db-L => live *D. balticum* culture; Db-U => uninoculated/abiotic *D. balticum* media. Fe to Mo ratios are 1:2, 1:1, or 2:1 as indicated for each sample in [Fe] series.

Table S5. TEM Mo, Fe, and S speciation percentage data.

Sample	Initial pH[b]	Ionic Strength (M)	Initial Mo Species[c]	Final pH[d]	Final $[Mo]_s$ (%)	Final $[Fe]_s$ (%)	Final $Fe:Mo_s$	Structure
Abiotic FeMoS experiments (from low to high pH)	4.34	0.01	MoO_4^{2-}	4.33	6.7 ± 1.49	2.27 ± 0.42	0.35 ± 0.20	Amorphous
	7.57	0.01	MoO_4^{2-}	7.73	1.34 ± 0.49	3.47 ± 0.76	2.77 ± 0.68	Amorphous
	10.97	0.01	MoO_4^{2-}	10.96	0.006 ± 0.007	7.65 ± 2.94	322.7 ± 234.3[d]	Amorphous
Dv-L[a]	6.71[e]	0.1	MoO_4^{2-}	6.88	0.52 ± 0.06	0.66 ± 0.23	1.23 ± 0.35	Amorphous
Dv-U[a]	7.11	0.1	MoO_4^{2-}	7.52	2.36 ± 0.00	2.40 ± 0.04	1.03 ± 0.00	Amorphous
Dv-L (Mo added before inoc.)	6.67[e]	0.1	MoO_4^{2-}	7.01	1.85 ± 0.61	1.55 ± 0.09	0.75 ± 0.27	Crystalline
Dv-L (Fe added before inoc.)	6.65[e]	0.1	MoO_4^{2-}	6.94	1.30 ± 0.92	7.29 ± 2.68	22.72 ± 35.92	Amorphous
Dv-L (TM added before inoc.)	6.70[e]	0.1	MoS_4^{2-}	7.03	0.59 ± 0.53	0.45 ± 0.13	2.93 ± 2.41	Amorphous
Dv-D[a] (Fe+Mo added to dead cell culture)	6.71[e]	0.1	MoO_4^{2-}	6.89	0.19 ± 0.09	0.96 ± 0.40	7.84 ± 5.76	Amorphous
Db-L	7.38[e]	0.7	MoO_4^{2-}	7.45	1.77 ± 0.03	2.97 ± 0.77	1.69 ± 0.46	Amorphous
Db-U	7.82	0.7	MoO_4^{2-}	7.90	2.68 ± 0.27	3.00 ± 0.31	1.12 ± 0.00	Amorphous
Db-L (Mo added before inoc.)	7.35[e]	0.7	MoO_4^{2-}	7.39	1.18 ± 0.00	5.03 ± 0.00	4.26 ± 0.00	Amorphous
Db-L (TM added before inoc.)	7.38[e]	0.7	MoS_4^{2-}	7.56	0.19 ± 0.14	4.09 ± 1.20	20.52 ± 11.56	Amorphous
Db-D (Fe+Mo added to dead cell culture)	7.36[e]	0.7	MoO_4^{2-}	7.49	0.23 ± 0.00	1.03 ± 0.00	4.48 ± 0.00	Amorphous

[a]Dv = D. vulgaris media/cultures; Db = D. balticum media/cultures; L => live cell-containing cultures; D => dead cell-containing cultures; U => uninoculated media ("abiotic" refers to samples prepared in buffered MQ water); Fe and Mo were added after 5mM sulfide was produced/added unless otherwise noted.
[b]Initial pH was taken after autoclaving and 5 mM sulfide addition/production.
[c]All experiments were run with 0.5 mM initial $[Mo]_{aq}$ and $[Fe]_{aq}$ (initial Fe:Mo of 1:1) and 5 mM initial $[S]_{aq}$ (for inoculated cultures, initial S species was sulfate; for abiotic/uninoculated samples, initial S was sulfide).
[d]Final pH was taken from supernatant after aging (i.e., experimental duration).
[e]Initial pH for these experiments was taken before inoculation/sulfide production via SRB growth.

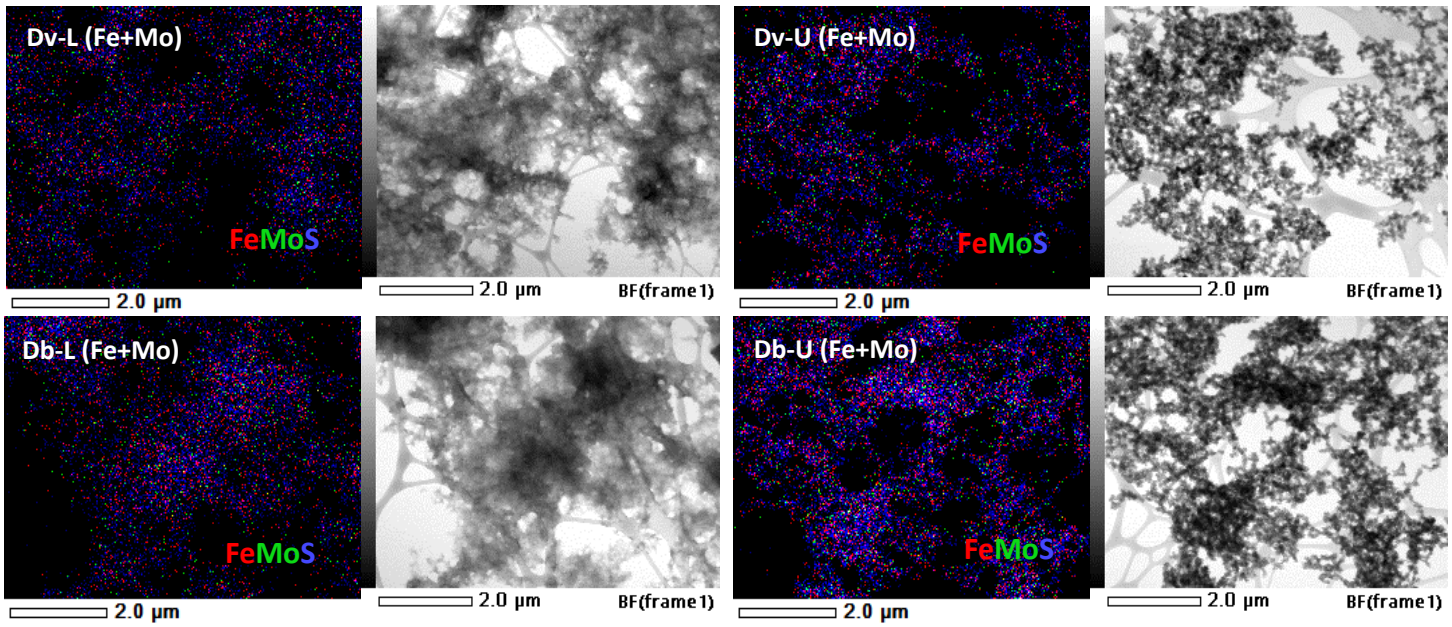

Figure S6. TEM EDS composite X-ray maps of representative FeMoS precipitates showing distribution of Fe (red), Mo (green), and S (blue). Abbreviations: Dv-L => live *D. vulgaris* culture; Dv-U => uninoculated/abiotic *D. vulgaris* media; Db-L => live *D. balticum* culture; Db-U => uninoculated/abiotic *D. balticum* media. Initial Fe to Mo ratios are 1:1.

S4. General XANES and EXAFS preparation and analyses

Samples were ground into a fine powder with a mortar and pestle and spread between two pieces of Kapton tape for X-ray absorption near edge structure (XANES) and extended X-ray absorption fine structure (EXAFS) analyses. Molybdenum K-edge XAS spectra were collected on the Bio-XAS-main beamline at room temperature at the Canadian Light Source (CLS) synchrotron in Saskatoon, Canada. This beamline has an energy resolution of $< 1 \times 10^{-4}$ eV with a flux $> 1 \times 10^{12}$ photons per second and a spot size of ~ 3 × 0.5 mm, focused using Rh-coated toroidal mirrors while a Si(220) double crystal monochromator selects the energy. The beamline is equipped with Ge-32 element fluorescence detectors, Soller slits, and a Zr6 fluorescence filter to increase the signal to noise ratio at the Molybdenum K-edge. Molybdenum K-edge XAS spectra were collected (3 scans per sample) over an energy range of –200 eV below the Mo K-edge (~20,000 eV) to k=15 $Å^{-1}$ at 10 eV steps in the pre-edge region (i.e., 19800–19970 eV), 0.5 eV steps in the XANES region (i.e., 19970–21000 eV), and 0.05 k in the EXAFS region (i.e., 21000 eV to 15 $Å^{-1}$). All spectra were collected with an internal reference (Mo foil) for calibration and alignment. Sample data are reported as edge-step normalized absorbance and were collected in fluorescence mode, while the Mo foil was measured in transmission mode. Background subtraction and normalization of Mo XAS data were performed using the Athena program in the Demeter software package (Ravel and Newville, 2005).

Raw scans were corrected for the total flux in I_0 and imported into Athena as μ(E) as fluorescence data. Replicate scans were aligned and merged. An E_0 value for each individual spectra was set as the highest point in the main peak of the first derivative. Due to the strong pre-edge peak associated with Mo(VI)-containing samples due to the Mo=O in molybdate, MoO_4^{2-} (Wagner et al., 2017), the E_0 value for these samples was set as the highest point on the peak associated with the main rising edge in μ(E), rather than the first peak in the first derivative. The pre-edge, post-edge, edge-step normalization range used the automatically selected lower and upper bounds. The normalization step was one arbitrary absorbance unit. Data normalized to the edge step are presented graphically. To plot the χ(k) and χ(R) space for the K-edge spectra, the R background was set to 1.0 with a k-weight of 2 and these values remained constant. The spline range for the R background function extended throughout the entirety of the dataset from 0-15 k. The forward Fourier transform k-range was set from 3.0-13.9 $Å^{-1}$ with a dk of 1 in the Hanning window. The backwards Fourier transform was from 1-3 with a dR of 0 in a Hanning window.

S5. Molybdenum XANES linear combination fitting (LCF) parameters

All XANES obtained were subject to linear combination fitting (LCF) using Athena to determine the average oxidation state of Mo in our samples. The LCF fitting range was carried out with normalized μ(E) spectra from -20 eV to +30 eV relative to the Mo K-edge (20,000 eV). Sample spectra were fit using endmember standards molybdate ($Mo^{VI}O_4^{2-}$), tetrathiomolybdate ($Mo^{VI}S_4^{2-}$), and molybdenite ($Mo^{IV}S_2$) with weights forced to sum to 1.0 and E_0 fixed. Fitting results and statistics (R factor and reduced chi-square values) are listed in Table S6. The Mo oxidation state was calculated using weighted average of standards that fit each sample, and the resulting values based on the XANES LCF data are in good agreement with the Mo oxidation states calculated for the same set of samples using XPS fitting. The average across all FeMoS samples is 4.33 ± 0.12 based on XANES LCF and 4.21 ± 0.13 based on XPS (both of these averages exclude the non-reduced, high pH sample, which is likely molybdate), indicating the predominance of fully reduced Mo(IV) in our FeMoS samples. The slightly higher Mo oxidation state calculated using LCF compared to that calculated via XPS is likely due to the lack of more structurally similar reduced Mo(IV) and/or Mo(V) standard(s) other than $Mo^{IV}S_2$ (e.g., Dahl et al., 2017). For this reason, we focus mainly on the Mo oxidation states calculated from XPS in the main text, which due to the high-resolution peak fitting based on Mo(IV), Mo(V), and Mo(VI) binding energies from previous literature, is likely more representative of the actual oxidation state of Mo in our samples.

S6. Molybdenum EXAFS fitting parameters

After processing data in Athena, the Artemis software was used to fit the EXAFS spectra (Ravel and Newville, 2005). The Mo-O, Mo-S, and Mo-Fe interatomic distances, sigma squared values, $S0^2$ values, and R-factors for the best fits of all EXAFS spectra, and alternative fits for the time series samples, are listed in Tables S7 and S8. The EXAFS fitting done using Mo-S and Mo-Fe single scattering paths in the $Fe(MoS_2)_2$ structure from Vaqueiro et al. (2002) and the Mo-O single scattering path in the MoO_2S_4 cofactor structure from Chrysochos et al. (2019). Best fits were obtained through fitting spectra from kmin = 3 to kmax = 14 and rmin = 1 to rmax = 3 with one Mo-O path and four Mo-S paths with the coordination number (N) set to 1 and change in half path length (ΔR) allowed to vary. Multiple Mo-S paths were used instead of one Mo-S path set at N = 4 because of the amorphous structure and presence of various sulfur species (S^{2-}, S_2^{2-}, and S_n^{2-}) in our FeMoS precipitates, which make the Mo-S bond lengths vary throughout the bulk precipitate (Helz et al., 1996; Bostick et al., 2003; Freund et al., 2016; Dahl et al., 2017; Vorlicek et al., 2018). The amplitude reduction factor ($S0^2$) was also allowed to vary for each fit. Alternative fits were run on time series samples, following methods of Dahl et al. (2017), with and without the Mo-Fe path and the Mo-O path to show the change in fit R-factor when these bonds are included and excluded (Table S8). These fits indicate that, for most samples, the best fit is obtained when one Mo-O and Mo-Fe bond are included in the model; however, it also emphasizes that the presence of O and Fe only slightly increase the quality of the fit based on R-factor. Thus, although there are potentially Mo-O and Mo-Fe bonds in the coordination environment of Mo in our FeMoS samples, the Mo-S bonds are much more significant and certain based on the EXAFS fits.

Table S6. Linear combination fitting (LCF) results and statistics.

Sample	$Mo^{VI}O_4^{2-}$, [a]	$Mo^{VI}S_4^{2-}$	$Mo^{IV}S_2$	Average Mo Oxidation State	Reduced chi-square	R factor
Abiotic FeMoS (low pH)	0.00	0.25	0.75	4.50 ± 0.18	0.0009	0.004
Abiotic FeMoS (neutral pH)	0.00	0.18	0.82	4.36 ± 0.23	0.0030	0.017
Abiotic FeMoS (high pH)	1.00	0.00	0.00	6.00 ± 0.00	0.0025	0.020
Dv-L (5 min)	0.00	0.17	0.83	4.34 ± 0.09	0.0006	0.003
Dv-L (24 h)	0.00	0.08	0.92	4.16 ± 0.08	0.0003	0.002
Dv-L (4 d)	0.00	0.19	0.81	4.38 ± 0.08	0.0005	0.003
Dv-L (8 d)	0.00	0.08	0.92	4.16 ± 0.08	0.0003	0.002
Dv-L (40+ d)	0.00	0.00	1.00	4.00 ± 0.00	0.0005	0.003
Dv-U (5 min)	0.08	0.11	0.81	4.38 ± 0.16	0.0006	0.003
Dv-U (24 h)	0.00	0.21	0.79	4.42 ± 0.07	0.0003	0.001
Dv-U (4 d)	0.00	0.18	0.82	4.36 ± 0.07	0.0003	0.002
Dv-U (8 d)	0.00	0.22	0.78	4.44 ± 0.07	0.0003	0.001
Dv-U (40+ d)	0.00	0.13	0.87	4.25 ± 0.07	0.0003	0.002
Dv-L (1:2 Fe:Mo)	0.00	0.20	0.80	4.40 ± 0.06	0.0004	0.002
Dv-L (1:1 Fe:Mo)	0.00	0.00	1.00	4.00 ± 0.00	0.0005	0.003
Dv-L (2:1 Fe:Mo)	0.00	0.18	0.82	4.36 ± 0.06	0.0004	0.002
Dv-U (1:1 Fe:Mo)	0.00	0.13	0.87	4.36 ± 0.07	0.0003	0.002
Dv-U (2:1 Fe:Mo)	0.00	0.20	0.80	4.40 ± 0.05	0.0003	0.001
Db-U (1:1 Fe:Mo)	0.00	0.17	0.83	4.34 ± 0.05	0.0002	0.001

[a]A value of 0.00 indicates that the contribution from the molybdate spectra in this fit was insignificant (< 0.05) and was excluded from the final fit.

Table S7. Best EXAFS fits for standards and fully aged samples. A denotes abiotic solutions (ionic strength = 0.01 M); low pH = 4.34 ± 0.04; neutral pH = 7.57 ± 0.06; high pH = 10.97 ± 0.02; Dv => *D. vulgaris* culture media (ionic strength = 0.1 M; pH = 7.01 ± 0.17) ; Db => *D. balticum* culture media (ionic strength = 0.1 M; pH = 7.76 ± 0.16); L denotes the presence of living cells; D denotes the presence of dead cells; U denotes uninoculated/no cells present.

Sample	**N**	**R_O (Å)**	**σ^2**	**N**	**R_{S1} (Å)**	**σ^2**	**N**	**R_{S2} (Å)**	**σ^2**	**N**	**R_{S3} (Å)**	**σ^2**	**N**	**R_{Fe} (Å)**	**σ^2**	**$S0^2$**	**R factor**
MoO_4^{2-}	4	1.77 ± 0.02	0.001													0.61 ± 0.03	0.020
MoS_4^{2-}				4	2.17 ± 0.01	0.001										0.64 ± 0.02	0.016
MoS_2				6	2.39 ± 0.01	0.001							6	3.15 ± 0.01[a]	0.003	0.71 ± 0.03	0.012
Abiotic FeMoS (low pH)	1	1.63 ± 0.03	0.04	1	2.35 ± 0.05	0.001	1	2.42 ± 0.09	0.008	2	2.48 ± 0.01	0.002	1	3.00 ± 0.03	0.01	1.22 ± 0.03	0.007
Abiotic FeMoS (neutral pH)	1	1.65 ± 0.04	0.04	1	2.32 ± 0.01	0.001	1	2.40 ± 0.01	0.002	2	2.51 ± 0.04	0.006	1	2.88 ± 0.05	0.02	0.99 ± 0.04	0.010
Abiotic FeMoS (high pH)	4	1.75 ± 0.03	0.001													1.36 ± 0.11	0.030
Dv-L (1:2 Fe:Mo)	1	1.65 ± 0.02	0.03	1	2.31 ± 0.01	0.006	1	2.34 ± 0.02	0.001	2	2.45 ± 0.04	0.001	1	2.95 ± 0.04	0.01	1.17 ± 0.04	0.010
Dv-L-(1:1 Fe:Mo)	1	1.65 ± 0.02	0.03	1	2.32 ± 0.01	0.01	1	2.36 ± 0.01	0.002	2	2.45 ± 0.06	0.002	1	2.90 ± 0.02	0.03	1.38 ± 0.04	0.008
Dv-L (2:1 Fe:Mo)	1	1.65 ± 0.02	0.03	1	2.33 ± 0.01	0.003	1	2.36 ± 0.01	0.001	2	2.49 ± 0.05	0.001	1	2.83 ± 0.05	0.04	1.25 ± 0.04	0.013
Dv-U (1:1 Fe:Mo)	1	1.65 ± 0.03	0.03	1	2.32 ± 0.02	0.008	1	2.36 ± 0.01	0.002	2	2.46 ± 0.05	0.002	1	2.88 ± 0.04	0.02	1.34 ± 0.04	0.007
Dv-U (2:1 Fe:Mo)	1	1.65 ± 0.02	0.04	1	2.33 ± 0.01	0.003	1	2.36 ± 0.01	0.001	2	2.49 ± 0.03	0.003	1	2.89 ± 0.04	0.02	1.24 ± 0.04	0.008
Db-U (1:1 Fe:Mo)	1	1.65 ± 0.02	0.04	1	2.33 ± 0.02	0.005	1	2.35 ± 0.02	0.001	2	2.48 ± 0.06	0.002	1	2.89 ± 0.03	0.02	1.28 ± 0.05	0.007

[a]Mo-Mo in molybdenite (MoS_2)

Table S8. Best and alternative EXAFS fits for the time series samples. All time series samples were conducted at a 1:1 initial aqueous Fe:Mo ratio in *D. vulgaris* (Dv) culture media. L in the sample name denote the presence of living cells; U denotes uninoculated solutions/the absence of cells.

Sample	N	R_O (Å)	σ^2	N	R_{S1} (Å)	σ^2	N	R_{S2} (Å)	σ^2	N	R_{S3} (Å)	σ^2	N	R_{Fe} (Å)	σ^2	$S0^2$	R factor
Dv-L (5 min)	1	1.65 ± 0.02	0.03	1	2.33 ± 0.01	0.005	1	2.36 ± 0.01	0.002	2	2.47 ± 0.04	0.002	1	2.71 ± 0.07	0.02	1.27 ± 0.06	0.009
Alternative fit	1	1.62 ± 0.03	0.03	1	2.32 ± 0.01	0.002	1	2.37 ± 0.01	0.001	2	2.49 ± 0.04	0.002				1.23 ± 0.05	0.013
Alternative fit				1	2.34 ± 0.03	0.001	1	2.35 ± 0.03	0.001	2	2.48 ± 0.05	0.002				1.05 ± 0.07	0.030
Dv-L (24 h)	1	1.65 ± 0.02	0.03	1	2.33 ± 0.01	0.005	1	2.36 ± 0.01	0.002	2	2.46 ± 0.03	0.002	1	2.88 ± 0.06	0.03	1.22 ± 0.04	0.006
Alternative fit	1	1.64 ± 0.02	0.03	1	2.32 ± 0.01	0.005	1	2.36 ± 0.01	0.001	2	2.48 ± 0.03	0.001				1.33 ± 0.05	0.008
Alternative fit				1	2.33 ± 0.02	0.001	1	2.37 ± 0.02	0.001	2	2.48 ± 0.04	0.001				1.07 ± 0.07	0.018
Dv-L (4 d)	1	1.65 ± 0.02	0.03	1	2.31 ± 0.01	0.003	1	2.35 ± 0.01	0.002	2	2.44 ± 0.04	0.002	1	2.89 ± 0.04	0.02	1.26 ± 0.05	0.014
Alternative fit	1	1.64 ± 0.04	0.04	1	2.33 ± 0.01	0.006	1	2.36 ± 0.01	0.001	2	2.46 ± 0.05	0.004				1.24 ± 0.05	0.015
Alternative fit				1	2.33 ± 0.02	0.006	1	2.36 ± 0.02	0.001	2	2.46 ± 0.05	0.004				1.15 ± 0.04	0.016
Dv-L (8 d)	1	1.65 ± 0.03	0.03	1	2.33 ± 0.01	0.008	1	2.39 ± 0.01	0.003	2	2.45 ± 0.04	0.002	1	2.88 ± 0.04	0.02	1.27 ± 0.04	0.006
Alternative fit	1	1.64 ± 0.03	0.03	1	2.32 ± 0.01	0.002	1	2.44 ± 0.01	0.0001	2	2.49 ± 0.04	0.0001				1.26 ± 0.06	0.011
Alternative fit				1	2.32 ± 0.03	0.001	1	2.43 ± 0.04	0.004	2	2.47 ± 0.07	0.003				1.11 ± 0.08	0.019
Dv-L (40+ d)	1	1.65 ± 0.02	0.03	1	2.32 ± 0.01	0.01	1	2.36 ± 0.01	0.002	2	2.45 ± 0.06	0.002	1	2.90 ± 0.02	0.03	1.38 ± 0.04	0.008
Alternative fit	1	1.64 ± 0.03	0.03	1	2.33 ± 0.01	0.003	1	2.37 ± 0.01	0.002	2	2.48 ± 0.05	0.001				1.33 ± 0.05	0.009
Alternative fit				1	2.33 ± 0.02	0.001	1	2.39 ± 0.01	0.002	2	2.47 ± 0.05	0.003				1.12 ± 0.07	0.020
Dv-U (5 min)	1	1.64 ± 0.02	0.02	1	2.31 ± 0.02	0.003	1	2.39 ± 0.02	0.001	2	2.47 ± 0.04	0.003	1	2.88 ± 0.06	0.02	1.31 ± 0.05	0.007
Alternative fit	1	1.64 ± 0.03	0.03	1	2.33 ± 0.02	0.003	1	2.36 ± 0.01	0.008	2	2.47 ± 0.04	0.001				1.37 ± 0.05	0.008
Alternative fit				1	2.31 ± 0.03	0.001	1	2.38 ± 0.03	0.001	2	2.47 ± 0.05	0.002				1.07 ± 0.09	0.030
Dv-U (24 h)	1	1.64 ± 0.02	0.03	1	2.32 ± 0.01	0.005	1	2.35 ± 0.01	0.001	2	2.47 ± 0.03	0.002	1	2.88 ± 0.05	0.02	1.25 ± 0.04	0.007
Alternative fit	1	1.65 ± 0.02	0.03	1	2.32 ± 0.02	0.003	1	2.39 ± 0.01	0.004	2	2.48 ± 0.04	0.002				1.41 ± 0.07	0.012
Alternative fit				1	2.33 ± 0.03	0.001	1	2.38 ± 0.02	0.002	2	2.49 ± 0.06	0.002				1.14 ± 0.09	0.021
Dv-U (4 d)	1	1.65 ± 0.02	0.05	1	2.30 ± 0.01	0.008	1	2.36 ± 0.01	0.001	2	2.46 ± 0.04	0.002	1	2.89 ± 0.05	0.02	1.29 ± 0.05	0.013
Alternative fit	1	1.67 ± 0.02	0.05	1	2.34 ± 0.01	0.002	1	2.35 ± 0.01	0.015	2	2.47 ± 0.04	0.001				1.43 ± 0.07	0.014
Alternative fit				1	2.34 ± 0.01	0.003	1	2.36 ± 0.01	0.002	2	2.49 ± 0.05	0.001				1.18 ± 0.06	0.017
Dv-U (8 d)	1	1.69 ± 0.04	0.03	1	2.32 ± 0.01	0.009	1	2.35 ± 0.01	0.002	2	2.45 ± 0.04	0.002	1	2.89 ± 0.04	0.02	1.25 ± 0.04	0.008
Alternative fit	1	1.65 ± 0.02	0.03	1	2.33 ± 0.01	0.004	1	2.38 ± 0.01	0.004	2	2.48 ± 0.05	0.001				1.34 ± 0.07	0.014
Alternative fit				1	2.33 ± 0.02	0.001	1	2.39 ± 0.03	0.003	2	2.48 ± 0.06	0.002				1.10 ± 0.09	0.025
Dv-U (40+ d)	1	1.65 ± 0.03	0.03	1	2.32 ± 0.02	0.008	1	2.36 ± 0.01	0.002	2	2.46 ± 0.05	0.002	1	2.88 ± 0.04	0.02	1.34 ± 0.04	0.007
Alternative fit	1	1.64 ± 0.02	0.03	1	2.32 ± 0.02	0.001	1	2.43 ± 0.02	0.002	2	2.49 ± 0.04	0.001				1.39 ± 0.07	0.013
Alternative fit				1	2.32 ± 0.02	0.001	1	2.39 ± 0.02	0.002	2	2.49 ± 0.04	0.002				1.16 ± 0.10	0.023

Supplementary References:

Bostick, B.C., Fendorf, S., Helz, G.R., 2003. Differential adsorption of molybdate and tetrathiomolybdate on pyrite (FeS2). Environ. Sci. Technol. 37, 285–291.

Chrysochos, N, Ahmadi, M., Wahlefeld, S., Rippers, Y., Zebger, I., Mroginski, M.A., Schulzke, C., 2019. Comparison of molybdenum and rhenium oxo bis-pyrazine-dithiolene complexes – in search of an alternative metal centre for molybdenum cofactor models. Dalton Trans. 48, 2701-2714.

Dahl, T.W., Chappaz, A., Hoek, J., McKenzie, C.J., Svane, S., Canfield, D.E., 2017. Evidence of molybdenum association with particulate organic matter under sulfidic conditions. Geobiol. 15, 311–323.

Freund, C., Wishard, A., Brenner, R.; Sobel, M., Mizelle, J., Kim, A., Meyer, D. A., Morford, J. A., 2016. The effect of a thiol-containing organic molecule on molybdenum adsorption onto pyrite. Geochim. Cosmochim. Acta 174, 222−235.

Helz, G.R., Miller, C.V., Charnock, J.M., Mosselmans, J.F.W., Pattrick, R.A.D., Garner, C. D., Vaughan, D.J., 1996. Mechanism of molybdenum removal from the sea and its concentration in black shales: EXAFS evidence. Geochim. Cosmochim. Acta 60, 3631–3642.

Herbert, R. B.; Benner, S. G.; Pratt, A. R.; Blowes, D. W., 1998. Surface chemistry and morphology of poorly crystalline iron sulfides precipitated in media containing sulfate-reducing bacteria. Chemical Geology 144, (1-2), 87-97.

Herrera, J.E. and Resasco, D.E., 2004. Loss of single-walled carbon nanotubes selectivity by disruption of the Co–Mo interaction in the catalyst. J. Catal. 221, 354.

Karthe, S., Szargan, R., Suoninen, E., 1993. Oxidation of pyrite surfaces: A photoelectron spectroscopic study. Appl. Surf. Sci. 72 (2), 157−170.

Lan, Y. and Butler, E.C., 2016. Iron-Sulfide-Associated Products Formed during Reductive Dechlorination of Carbon Tetrachloride. Environ. Sci. Technol. 50, 11, 5489–5497.

Miller, N., Dougherty, M., Du, R., Sauers, T., Yan, C., Pines, J.E., Meyers, K.L., Y M. Dang, Y.M., Nagle, E., Ni, Z., Pungsrisai, T., Wetherington, M.T., Vorlicek, T.P., Plass, K.E., Morford, J.L., 2020. Adsorption of Tetrathiomolybdate to Iron Sulfides and Its Impact on Iron Sulfide Transformations. ACS Earth Space Chem. 4, 2246−2260.

Muijsers, J.C., Weber, T., van Hardeveld, R.M., Zandbergen, H.W., Neimantsverdriet, J.W., 1995. Sulfidation Study of Molybdenum Oxide Using MoO3/SiO2/Si(100) Model Catalysts and MoIV3-Sulfur Cluster Compounds. J. Catal. 157, 698.

Mullet, M.; Boursiquot, S.; Abdelmoula, M.; Genin, J. M.; Ehrhardt, J. J., 2002. Surface chemistry and structural properties of mackinawite prepared by reaction of sulfide ions with metallic iron. Geochim Cosmochim Acta 66, (5), 829-836.

Nesbitt H.W., Muir I.J., 1994. X-ray photoelectron spectroscopic study of a pristine pyrite surface reacted with water vapour and air. Geochim. Cosmochim. Acta. 58, 4667–4679.

Supplementary References:

Nesbitt, H., Scaini, M., Höchst, H., Bancroft, G., Schaufuss, A., Szargan, R., 2000. Synchrotron XPS evidence for Fe2+−S and Fe3+−S surface species on pyrite fracture-surfaces, and their 3D electronic states. Am. Mineral. 85 (5−6), 850−857.

Phillips et al., 2023 Phillips, R.F., Singerling, S., Leng, W., Xu, J., 2023. Significance of pH and iron-sulfur chemistry for molybdenum sequestration under sulfidic conditions. Chemical Geology 638, 121702.

Poulton, S.W., 2003. Sulfide oxidation and iron dissolution kinetics during the reaction of dissolved sulfide with ferrihydrite. Chem. Geol. 202 (1−2), 79−94.

Qi, D., Duan, A., Zhao, Z., Wu, H., Fan, H., Fang, H., Li, J., Jiang, G., Liu, J., Wei, Y., Zhang, X., 2015. Catalytic performance and sulfidation behaviors of CoMo/Beta-MCM-48 catalysts prepared with citric acid for FCC gasoline hydroupgrading. S. Porous Mater, 22:127–135.

Ravel, B. and Newville, M., 2005. ATHENA, ARTEMIS, HEPHAESTUS: data analysis for X-ray absorption spectroscopy using IFEFFIT. J Synchrotron Radiat. (Pt 4): 537-41. PMID: 15968136.

Sanders, A.F.H., Jong, A.M., de Beer, V.H.J., van Veen, J.A.R, Niemantsverdriet, J.W., 1999. Formation of cobalt–molybdenum sulfides in hydrotreating catalysts: a surface science approach. Appl. Surf. Sci. 144–145, 380–384.Seo et al., 2015;

Seo, B., Jung, G.Y., Sa, Y.J., Jeong, H.Y., Cheon, J.Y., Lee, J.H., Kim, H.Y., Kim, J. C.; Shin, H.S., Kwak, S.K., Joo, S.H., 2015. Monolayer-Precision Synthesis of Molybdenum Sulfide Nanoparticles and Their Nanoscale Size Effects in the Hydrogen Evolution Reaction. ACS Nano 9, 3728−3739.

Seo, B., Jung, G.Y., Lee, S.J., Baek, D.S., Sa, Y.J., Ban, H.W., Son, J.S., Park, K., Kwak, S.K., Joo, S.H., 2020. Monomeric MoS42-- Derived Polymeric Chains with Active Molecular Units for Efficient Hydrogen Evolution Reaction. ACS Catal., 10, 652– 662.

Vaqueiro, P., Kosidowski, M. L., Powell., A.V., 2002. Structural Distortions of the Metal Dichalcogenide Units in AMo2S4 (A = V, Cr, Fe, Co) and Magnetic and Electrical Properties. Chem. Mater. 14, 3, 1201–1209.

Vorlicek, T.P., Helz, G.R., Chappaz, A., Vue, P., Vezina, A., Hunter, W., 2018. Molybdenum burial mechanism in sulfidic sediments: iron-sulfide pathway. ACS Earth Space Chem. 2, 565–576.

Wan, M.; Shchukarev, A.; Lohmayer, R.; Planer-Friedrich, B.; Peiffer, S., 2014. Occurrence of surface polysulfides during the interaction between ferric (hydr)oxides and aqueous sulfide. Environ. Sci. Technol. 48, (15), 8932-8932.

Weber, Th., Muijsers, J.C., Niemantsverdriet, J.W., 1995. Structure of amorphous MoS3. J. Phys. Chem. 99, 9194−9200.

Weber, T.; Muijsers, J.C., van Wolput, J.H.M.C.; Verhagen, C.P.J.; Niemantsverdriet, J.W., 1996. Basic reaction steps in the sulfidation of crystalline MoO3 to MoS2, as studied by X-ray photoelectron and infrared emission spectroscopy. J. Phys. Chem. 100, 14144−14150.